Developmental Biology xxx (xxxx) xxx

Contents lists available at ScienceDirect

Developmental Biology

journal homepage: www.elsevier.com/locate/developmentalbiology

Synchronized tissue-scale vasculogenesis and ubiquitous lateral sprouting underlie the unique architecture of the choriocapillaris

Zaheer Ali [a], Dongmei Cui [b], Yunlong Yang [c,d], Dhani Tracey-White [e], Gabriela Vazquez-Rodriguez [f], Mariya Moosajee [e], Rong Ju [b], Xuri Li [b], Yihai Cao [g], Lasse D. Jensen [a,*]

[a] Division of Cardiovascular Medicine, Department of Medical and Health Sciences, Linköping University, Linköping, Sweden
[b] Zhongshan Ophthalmic Center, State Key Laboratory of Ophthalmology, Sun Yat-sen University, Guangzhou, PR China
[c] Department of Cellular and Genetic Medicine, School of Basic Medical Sciences, Fudan University, Shanghai 200032, PR China
[d] Institute of Pan-vascular Medicine, Fudan University, Shanghai 200032, PR China
[e] Department of Ocular Biology and Therapeutics, UCL Institute of Ophthalmology, London, UK
[f] Department of Oncology and Department of Clinical and Experimental Medicine, Linköping University, Linköping, Sweden
[g] Department of Microbiology, Tumor and Cell Biology, Karolinska Institutet, Stockholm, Sweden

ARTICLE INFO

Keywords:
Choriocapillaris
Vasculogenesis
Angiogenesis
Zebrafish
Development

ABSTRACT

The choriocapillaris is an exceptionally high density, two-dimensional, sheet-like capillary network, characterized by the highest exchange rate of nutrients for waste products per area in the organism. These unique morphological and physiological features are critical for supporting the extreme metabolic requirements of the outer retina needed for vision. The developmental mechanisms and processes responsible for generating this unique vascular network remain, however, poorly understood. Here we take advantage of the zebrafish as a model organism for gaining novel insights into the cellular dynamics and molecular signaling mechanisms involved in the development of the choriocapillaris. We show for the first time that zebrafish have a choriocapillaris highly similar to that in mammals, and that it is initially formed by a novel process of synchronized vasculogenesis occurring simultaneously across the entire outer retina. This initial vascular network expands by un-inhibited sprouting angiogenesis whereby all endothelial cells adopt tip-cell characteristics, a process which is sustained throughout embryonic and early post-natal development, even after the choriocapillaris becomes perfused. Ubiquitous sprouting was maintained by continuous VEGF-VEGFR2 signaling in endothelial cells delaying maturation until immediately before stages where vision becomes important for survival, leading to the unparalleled high density and lobular structure of this vasculature. Sprouting was throughout development limited to two dimensions by Bruch's membrane and the sclera at the anterior and posterior surfaces respectively. These novel cellular and molecular mechanisms underlying choriocapillaris development were recapitulated in mice. In conclusion, our findings reveal novel mechanisms underlying the development of the choriocapillaris during zebrafish and mouse development. These results may explain the uniquely high density and sheet-like organization of this vasculature.

1. Introduction

The choroidal and retinal vasculatures of the eye are critical for providing nutrients to support the extremely metabolically active photoreceptors, and other retinal cell types, thereby enabling vision in vertebrates (Luo et al., 2013). On the other hand, ectopic formation of the ocular vasculatures during development or in adults is intimately involved in vision disorders including retinopathy of pre-maturity (ROP), diabetic retinopathy (DR) and age-related macular degeneration (AMD) (Luo et al., 2013; Cao et al., 2008, 2010). The latter is the most prevalent and the most common cause of blindness today. Both hyaloid vessels (which are later replaced by the retinal vessels) and choroidal vessels form during early stages of embryonic development (Kaufman et al., 2015; Heinke et al., 2012; Ellertsdottir et al., 2010; Hashiura et al., 2017). Although the development of the hyaloid and retinal vessels have been intensely studied in various animal models, the development of the

* Corresponding author. Linköping University, IMH, Campus US, Entrance 68, Pl. 08, SE-58185, Linköping, Sweden.
E-mail address: lasse.jensen@liu.se (L.D. Jensen).

https://doi.org/10.1016/j.ydbio.2019.02.002
Received 12 September 2018; Received in revised form 27 January 2019; Accepted 10 February 2019
Available online xxxx

choroidal vasculature is still poorly understood. The choriocapillaris is the innermost part of the choroidal vasculature, located at close proximity to the retina, immediately posterior to the retinal pigment epithelium (RPE) and Bruch's membrane (BM). The choriocapillaris has the highest density of any vasculature in the body and its unique 2D, lobular, sheet-like morphology (Lutty and McLeod, 2018) further suggests that the development of the choriocapillaris may follow a unique trajectory or be regulated by unique mechanisms. Furthermore, ectopic growth of choroidal vessels during embryonic development or in adults is intimately coupled to the most common vision-threatening diseases including AMD and myopia respectively (Hashiura et al., 2017; Zhang and Wildsoet, 2015). It is plausible that understanding the mechanisms underlying choriocapillaris development may also provide deeper insights into the development of these diseases.

While snap shots of developing choriocapillaris, as well as other ocular vasculatures, in humans have recently been summarized in an excellent review of existing histological data by Lutty and McLeod (Lutty and McLeod, 2018), this work does not address the key issue of how the choriocapillaris develops its unique density or structure, and provides little insights into the highly dynamic cellular behaviors underlying morphogenesis of the vasculature. Using vascular casting, Djonov and collegues suggested that choriocapillaris development in chicken occurred through intussusceptive arborization (Djonov et al., 2000), while sprouting seemed to be the main mechanism in mice (Chan-Ling et al., 2011) and humans (Lutty and McLeod, 2018). Chan-Ling et al. suggested that mouse choriocapillaries lacks robust mural cell coverage during development (Chan-Ling et al., 2011), but the human choriocapillaris was reported to recruit mural cells and mature relatively early during development (Lutty and McLeod, 2018). As such, the current evidence, which mainly focuses on analyzing small areas of the choriocapillaris, usually from sagittal sections that does not allow studies of their 2D shape and only on one or a few developmental stages, is inconsistent and contradicting. In order to understand the development of the choriocapillaris, an animal model which allows longitudinal visualization of the entire choriocapillaris in the same (living) animal, and in high spatial 3D-detail, is needed.

In the past decade, zebrafish have emerged as an excellent model organism for investigating molecular and cellular mechanisms involved in vascular development. Zebrafish offer several benefits over other animal systems such as rapid, extra-uterine development of transparent embryos and their high genetic and pharmacologic amenability (Jensen et al., 2011). We and others have previously demonstrated that the zebrafish is a powerful system for understanding mechanisms underlying hyaloid vessel development (Jensen et al., 2015; Alvarez et al., 2007, 2009) and adult retinal vessel growth related to diabetic retinopathy (Cao et al., 2008, 2010; Alvarez et al., 2010). The formation of large, external choroidal vessels and the vasculature of the outflow tract have also been described in the zebrafish (Hashiura et al., 2017; Gray et al., 2009), but a detailed study on the cellular and molecular mechanisms involved in choriocapillaris formation is still lacking.

Here, we for the first time provide novel and detailed insights into the events leading to the formation of the choriocapillaris, which underlies its unique morphological and physiological characteristics. We show that the choriocapillaris is initially formed by synchronized vasculogenesis involving the fusion of endothelial cell clusters (so-called blood islands) homogeneously interspersed throughout the entire outer retina. This was followed by sustained and ubiquitous angiogenic expansion throughout the choriocapillaris due to VEGF-induced delayed maturation, which was finally relieved at 120 h post fertilization (hpf) resulting in rapid maturation and inhibition of sprouting leading to an adult-like choriocapillaris. Other choroidal vasculatures including a rete mirabile also found in other vertebrates, developed during adolescence. The role of VEGF-induced ubiquitous and sustained sprouting coupled to delayed maturation was recapitulated in mice, suggesting that this mechanism is conserved in mammals.

2. Material and methods

2.1. Zebrafish strains and their maintenance

Tg (fli1a:EGFP)^{y1}, Tg (kdrl:EGFP)^{s843}, Tg (kdrl:DsRed2)^{pd27}, Tg (acta2:EGFP)^{ca7}, Tg (tagln:EGFP)^{p151} and Tg (gata1a:DsRed2)^{sd2} transgenic strains (Lawson and Weinstein, 2002; Kikuchi et al., 2011; Jin et al., 2005; Seiler et al., 2010; Whitesell et al., 2014; Traver et al., 2003) were obtained from ZIRC, Oregon. Tg (fli1ep:Gal4FF)^{ubs3} (Zygmunt et al., 2011), Tg (UAS:RFP) and Tg (UAS:EGFP-UCHD)^{ubs18} (Sauteur et al., 2014) transgenic strains were generated in the Affolter laboratory and the Hif1aa-/-;Hif1ab-/- (Gerri et al., 2017) and Hsp70:VEGFAA-DN (Marin-Juez et al., 2016) zebrafish lines were generated in the Stainier laboratory. All strains and double or triple transgenic crosses between these strains were maintained at the Zebrafish facility at Linköping University, Linköping, Sweden following standard protocols (Rouhi et al., 2010; Jensen et al., 2012). All the experimental procedures have been previously approved by the Linköping animal ethics committee.

2.2. Zebrafish euthanasia and dissection

Zebrafish were anesthetized with 0.04% MS-222 (Ethyl 3-aminobenzoate methane sulfonic acid salt 98%, Sigma Aldrich) and fixed with 4% PFA (Sigma Aldrich) for 30 min at room temperature. The eyes were removed and dissected using watchmakers' forceps (Dumont #5) under a dissection microscope (Nikon SMZ 1500). The eyes were flat mounted on glass slides in Vectashield mounting medium (H-1000 Vector laboratories).

2.3. Vegfaa-DN treatment

Embryos generated from in-crosses of homozygous Hsp70:VEGFAA-DN transgenic zebrafish were incubated at 37 °C for 1 h per day at 1, 2, 3 and 4 days post fertilization (dpf) to induce persistent expression of dominant negative VEGF-A.

2.4. Time lapse analysis

Embryos at different age groups were incubated in a mixture of MS-222 (Ethyl 3-aminobenzoate methane sulfonic acid salt 98%, Sigma Aldrich) 25 μg/ml and 0.5% low melting agarose (Sigma Aldrich). The embryos were mounted in the glass bottom microwell dishes, (MatTek Corporation). Time-lapse image series were taken with 15 or 20 min interval between each frame using a confocal microscope (LSM 700 inverted, Zeiss, USA). The z-stacks images have been analyzed in Image J (NIH) or using the Imaris software (Bitplane, Switzerland).

2.5. Transmission electron microscopy (TEM)

Wildtype zebrafish embryos (3, 4, 5 dpf) were fixed in 2% paraformaldehyde-2% glutaraldehyde prior to incubation in 1% osmium tetroxide-1% potassium ferrocyanide. Following dehydration with an ethanol series and then incubation in propylene oxide, the zebrafish/retinas were embedded in EPON® resin (Polysciences, Inc., Warrington, PA) following manufacturer's instructions. Using a Reichert Ultracut S, 70-nm serial sections were cut and mounted on formvar coated copper grids and stained with Reynold's lead citrate. The grids were then examined on a JEOL 1010 TEM and images captured using a Gatan Orius SC1000B charge-coupled device camera. At least three zebrafish for each time point were used for examination in each experiment. Montaged images of semi-full-length retina were generated using low-magnification images in Microsoft Image Composite Editor. Photoshop was used to edit all other high magnification images.

2.6. Histology

Wildtype zebrafish retinas (1 month post fertilization (mpf) and adult (6 mpf)) were fixed in 4% paraformaldehyde prior to dehydration with an ethanol series. The zebrafish/retinas were then embedded in JB-4® Plus resin (Polysciences, Inc., Warrington, PA) following manufacturer's instructions. Using a Leica RM 2065 microtome, 7 μM serial sections were collected and stained with 1% toluidine blue. Sections were imaged on a Zeiss LSM510 upright microscope with Axiocam MRc digital camera. Image J was used to edit all images collected.

2.7. Mouse choroid whole-mount assay

BALB/c albino mouse eyes were enucleated following exposure to a lethal dose of CO2. After removal of extraocular muscles and connective tissues, the eye balls were fixed in 4% PFA for 24 h at 4 °C. During dissection, the conjunctiva, cornea, lens, iris, and retina were removed. Tissues containing choroids, sclera, and part of retinal non-pigmented epithelium were prepared for the whole-mount immunofluorescence staining. The tissues were digested with proteinase K (20 μg/mL), followed by incubation with a rat anti-mouse CD31 monoclonal antibody at 4 °C overnight. After rigorous rinsing, blood vessel endothelial cells were detected using secondary goat-anti-rat IgG antibodies conjugated with fluorescent Alexa 555 (Invitrogen). Tissues were flattened and mounted in Vectashield mounting medium (Vector Laboratories) and analyzed under a Nikon C1 Confocal microscope (Nikon Corporation). By scanning five to six layers (with 4–5 μm between adjacent layers) for each collection, 3D images of each collection were assembled using a confocal microscope software program. The images were further analyzed using Adobe Photoshop CS2 (Adobe).

2.8. Treatment with VEGF and VEGFR blockades

Pregnant BALB/c albino mice were kept in separate cages and maintained on a 12 h light/dark cycle throughout the experiment. Pregnant mice were treated with an anti-VEGFR2 monoclonal antibody (DC101, ImClone Systems, 5 mg/kg, IP, twice per week), or an IgG control antibody (10500C, Invitrogen, 5 mg/kg, IP, twice per week) starting at embryonic day E12 (n = 2 litters per group). Fetus were collected at embryonic day E16. Eyes were fixed and stained as described above.

2.9. Statistics

Results were generated in an un-blinded fashion and shown as means+/-SEM from at least three independent experiments. Statistical comparisons between two individual data sets were made using two-tailed, unpaired students t-test assuming equal variance between the groups. If nothing else is mentioned, comparisons have been made towards the control group (the left-most group in all the graphs) or between multiple data sets using single factor ANOVA. Significance are indicated using the following symbols when comparing two individual data sets in the graphs: * ($p < 0.05$), ** ($p < 0.01$) and *** ($p < 0.001$) with n-values as indicated in the figure legends. Healthy embryos were randomly allocated from a combined pool of embryos to each experimental group at the beginning of all experiments.

3. Results

3.1. Early development of the choriocapillaris in zebrafish follows synchronized vasculogenesis

To investigate the development of the choriocapillaris in high spatiotemporal detail in zebrafish, we took advantage of the Fli1a:EGFP strain in which EGFP is specifically expressed in the endothelial cells (Lawson and Weinstein, 2002). To improve visualization of the choroid, we developed a new mounting technique whereby the fish/eyes were mounted such that the posterior/scleral side of the eye was facing the objective of the microscope. Using this technique, we found that the development of the choriocapillaris begins at 18 hpf, roughly at the same time as the development of the hyaloid artery (HA) and optic artery (OA), by recruitment of single endothelial cells budding off from the developing cranial division of the internal carotid artery (CrDi) and primordial midbrain channel (PMBC) and migrating into sub-retinal area of the eye field (Fig. 1A and Supplemental Video 1). The recruitment of ECs from the CrDi and PMBC continued between 18 and 24 hpf, coinciding with the sprouting and growth of the dorsal and nasal radial vessels (DRV and NRV respectively) (Fig. 1B and Supplemental Video 2). At approximately 24 hpf, the outer eye field was completely populated with homogeneously interspaced single ECs. Choriocapillaris ECs (ccECs) continue to migrate within the eye field, leading to clustering of ccECs and formation of structures reminiscent of blood islands (Fig. 1A). By ~36 hpf ccECs projections had formed, which connected adjacent blood islands. These connections matured by 48 hpf to non-perfused vascular chords which became lumenized by 72 hpf (Fig. 1A). Throughout the process of establishing the initial choriocapillaris, the events were synchronized and occurred simultaneously throughout the entire outer eye field. This synchronization was enabled by the initial recruitment and regular interspersion of ccECs, and drove the formation of the characteristic honeycomb shape of the choriocapillaris at 72 hpf.

Supplementary video related to this article can be found at https://doi.org/10.1016/j.ydbio.2019.02.002.

3.2. Sprouting angiogenesis is required for choriocapillaris growth in zebrafish

The continuous expansion of the choriocapillaris, similar to its formation, involved the entire vasculature, leading to homogeneously and progressively increasing vascular density between 48 and 120 hpf (Fig. 1A, D). Using time-lapse confocal microscopy, we observed that this growth was achieved mainly through angiogenic sprouting and flow-mediated remodeling of the vascular morphology. Surprisingly nearly all ECs seemed to participate in the sprouting process, suggesting that the inhibition of tip-cell phenotypes in neighboring ECs seen in other vascular beds did not apply to the choriocapillaris. The ubiquitous and persistent sprouting resulted in the formation of an increasing number of thinner interstitial foci that could easily be interpreted as intussusceptive pillars (Fig. 1A and C and Supplemental Video 3 and 4). To elaborate on the role of intussusception during choriocapillaris development, we performed 3D surface rendering of Z-stack confocal data (Fig. 1E). A progressively increasing number of incomplete and anastomosed endothelial luminal processes, resembling immature intussusceptive pillars, were clearly apparent at 72, 96 and 120 hpf (Fig. 1E), suggesting that intussusception might be important for the expansion of the choriocapillaris. In the time-lapse videos, however, we could not detect the formations of persistent, “round holes” in the endothelium as a readout of intussusceptive pillar maturation (Supplemental video 4) in contrast to what was described previously in birds (Djonov et al., 2000). The continuous growth and remodeling of the choriocapillaris until 120 hpf was further demonstrated by the presence of longitudinal actin stress fibers in the ECs at 72 and 96 hpf, consistent with the sustained sprouting of this vasculature (Supplemental Fig. 1). At 120 hpf, however, the actin cytoskeleton was more dispersed along cortical networks consistent with a mature phenotype of the choriocapillaris endothelium at this stage (Supplemental Fig. 1). Taken together, this data suggests that the choriocapillaris expands by sustained, ubiquitous sprouting angiogenesis throughout early development culminating in rapid maturation at 120 hpf (Fig. 1F).

Supplementary video related to this article can be found at doi: 10.1016/j.ydbio.2019.02.002.

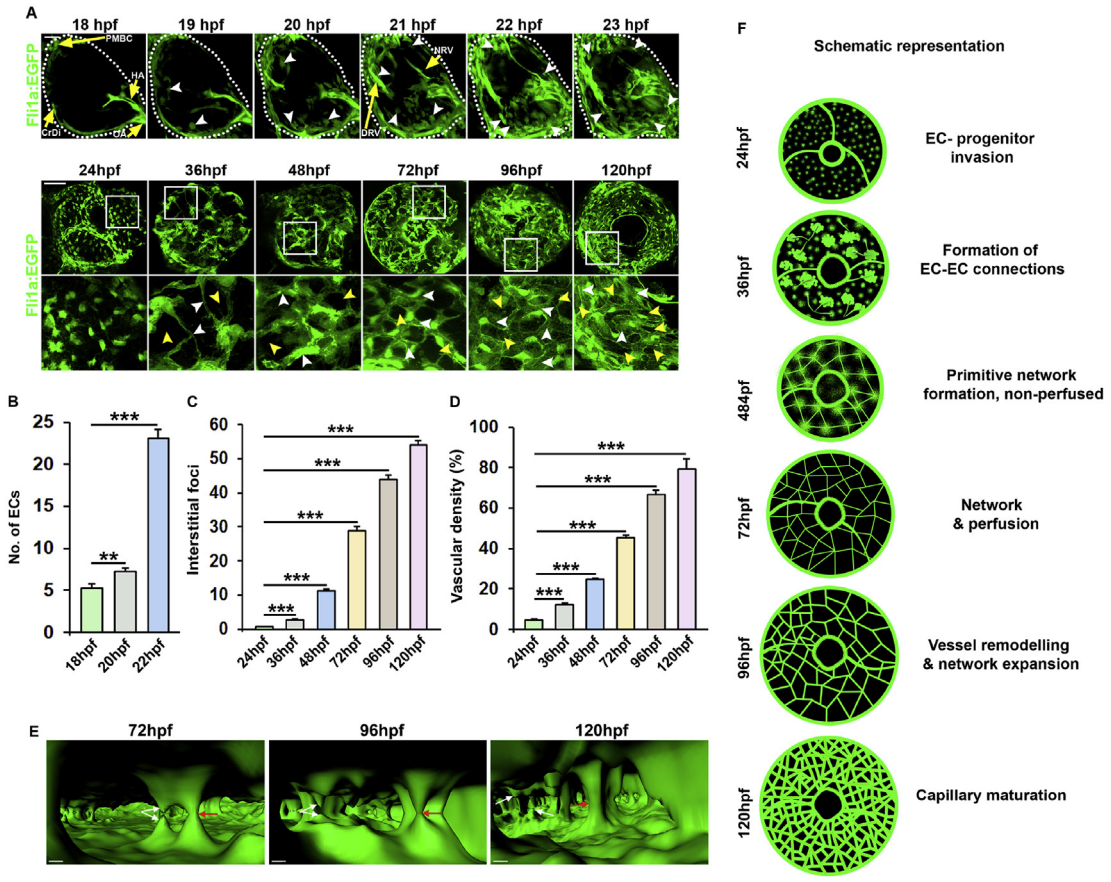

Fig. 1. Early development of the choriocapillaris in zebrafish. A: Time lapse confocal micrographs of the developing choriocapillaris (vessels shown in green) of the outer eye field in *Fli1a*:EGFP embryos at 18–23 h post fertilization (hpf, top row) and 24–120 hpf (lower row). Boxed regions are shown in magnified images below. Yellow arrows point to the indicated vessel structures, yellow arrowheads points to the avascular area or interstitial foci while white arrowheads points to endothelial cells or vessels. The dotted line indicates the eye field. Size bars indicates 50 μm in each image. CrDI: Cranial division of internal carotid artery, HA: Hyaloid artery, OA: Optic artery, PMBC: Primordial midbrain channel. DRV: Dorsal radial vessel. NRV: Nasal radial vessel. **B:** Quantifications of the number of the endothelial cells in the experiment shown in A. n = 10–15 embryos, **: $p < 0.01$ ***: $p < 0.001$. **C:** Quantification of the number of interstitial foci in the experiment shown in **A**. n = 10–15 embryos, ***:$p < 0.001$. **D:** Quantification of the vascular density of choriocapillaris in the experiment shown in **A**. n = 10–15 embryos, ***:$p < 0.001$. **E:** Imaris 3D rendering images of the choriocapillaris showing the lumen of CCs of complete intussusceptive pillars (red arrow) and incomplete pillars (white arrows) from 72, 96 and 120 hpf. Size bar indicates 10 μm. hpf: hours post fertilization. **F:** Scheme illustrating the development of choriocapillaris from 24 hpf to 120 hpf. Development of the choriocapillaris begins with the invasion of the endothelial cells via the PMBC and CrDi at 18–24 hpf. At 36 hpf the endothelial cells forms aggregates (blood islands) interconnected by thin processes (EC-EC connections), leading to formation of a primitive, non-lumenized vasculature at 48 hpf. The choriocapillaris become perfused at 72 hpf but remains actively expanding until maturation occurs at 120 hpf.

3.3. The choriocapillaris is a secondary hematopoietic organ during early development

It has been suggested that erythrocytes develop within blood islands in both hyaloid and choroidal vasculatures during early embryonic development (Lutty and McLeod, 2018). Using kdrl:EGFP; gata 1:DsRed double transgenic zebrafish, we found that erythrocytes co-developed with endothelial cells during the early stages of blood island formation and vasculogenesis in the choriocapillaris, leading to the formation of blood associated with the vessels even before their lumenization (Fig. 2A). Following lumenization and onset of perfusion at 72 hpf (Fig. 2C), however, we observed a sharp increase in the blood content, which was further elevated between 72 and 120 hpf (Fig. 2A and B). As other ocular vasculatures (including the hyaloid vessels) developed through angiogenesis, we did not see any evidence of blood formation outside of the choriocapillaris, suggesting that this vasculature provides additional erythroblasts during early embryonic development. Compared to the size of the hemogenic endothelium in the aorta and the caudal hematopoietic plexis, these findings suggest that the choriocapillaris may be an important hematopoietic tissue at least during early development.

3.4. Permeability of the choriocapillaris is maintained until late stages of development

As suggested by the lumenization of the choriocapillaries by 72 hpf, we found using intra-venous injection of rhodamine-conjugated dextran that the choriocapillaries initially became perfused by 72 hpf (Fig. 2C). The percentage of perfused choriocapillaries increased throughout development more than doubling between day three and four and increased an additional 50% between day four and five (Fig. 2C and D). On the other hand, leakiness of the choriocapillaris was maintained in the first four days despite increased perfusion, only dropping 17% between day two and three and 9% between day three and four (Fig. 2C and E). On day five, however, the vasculature had matured and leakiness dropped to approximately half of that on day four. These findings are therefore consistent with delayed maturation of the choriocapillaris during the first four days, which then rapidly matures at 120 hpf.

3.5. Sprouting of the choriocapillaris coincides with Bruch's membrane formation

To understand the cause of the two-dimensional-morphology of the

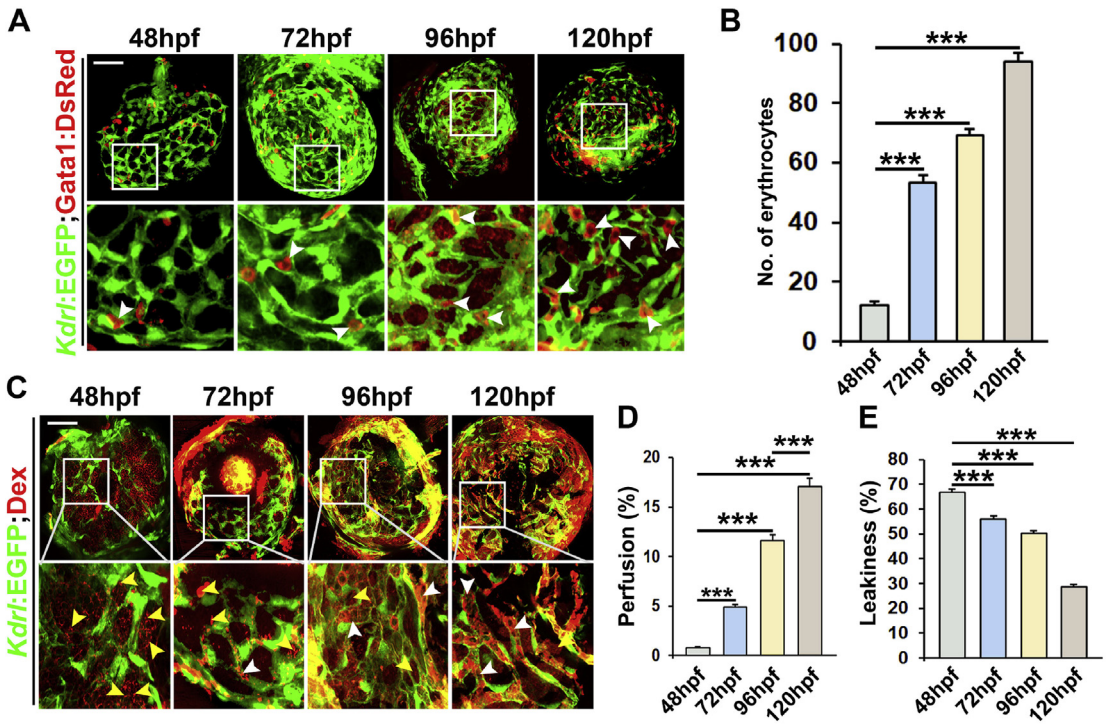

Fig. 2. Maturation of choriocapillaris leads to increased perfusion and reduced leakage. A: Confocal micrographs of the posterior eye of Kdrl:EGFP; Gata1:DsRed double transgenic embryos (endothelium shown in green and erythroblasts shown in red) at 48–120 hpf. Boxed regions are shown in magnified images below. White arrowheads points to erythrocytes. Size bar indicates 50 μm hpf, hours post fertilization. **D:** Quantification of the number of erythrocytes in the choriocapillaris between 48 and 120 hpf from the experiment shown in **A**. n = 10–15 embryos, ***:p < 0.001. **C:** Confocal micrographs of Kdrl:EGFP embryos (endothelium shown in green) at different time points between 48 and 120 hpf, 1 h after injection with rhodamine-conjugated 70 kDa dextran via the common cardinal vein (dextran (Dex) shown in red). Boxed regions are shown in magnified images below. Yellow arrowheads points to dextran leaked into the avascular area while white arrowheads points to dextran contained within the vascular lumen. Size bar indicates 50 μm. **D:** Quantification of perfusion in the choriocapillaris between 48 and 120 hpf. n = 10–15 embryos, ***:p < 0.001. **E:** Quantification of the dextran leakage between 48 and 120hpf. n = 10–15 embryos, ***:p < 0.001.

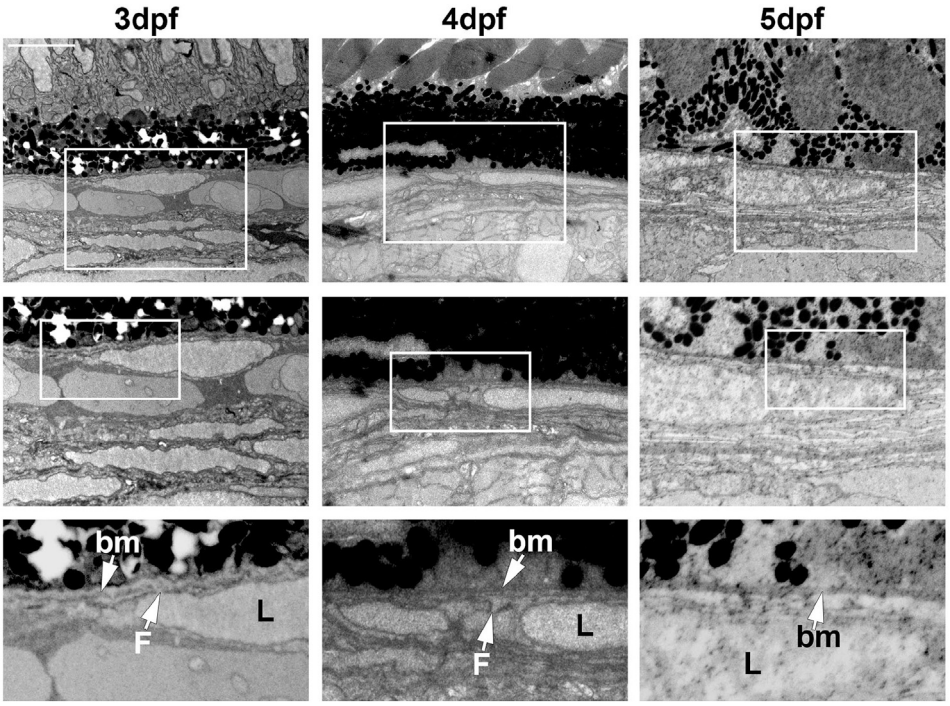

Fig. 3. Ultrastructure analysis of the choriocapillaris over development. Transmission electron micrographs (TEM) of 3–5 days post fertilization (dpf) zebrafish outer retina and choroid. Boxed regions are shown in the magnified images below. Bm: Bruch's membrane, F. Fenestration, L. Lumen. Size bar indicates 5 μm.

choriocapillaris and its maturation in higher structural detail, we analyzed the ultrastructure of the endothelium and adjacent Bruch's membrane/RPE and sclera. On day three, when robust sprouting was observed in the choriocapillaris, Bruch's membrane had already formed and provided a shield, preventing sprouting into the neuroretina. The RPE was however sparse and poorly differentiated at this stage, as many RPE cells were hypochromatic (Fig. 3 and Supplemental Fig. 2). The choriocapillaris was heavily fenestrated and no tight junctions or vascular mural cells could be observed, consistent with the lack of maturation. Some photoreceptor outer segments had reached the RPE, but the density was low (Fig. 3 and Supplemental Fig. 2). On day 4 on the other hand a well differentiated and dense RPE associated with high density photoreceptor outer segments was apparent in the entire outer retina (Supplemental Fig. 3). Bruch's membrane was similarly more defined and had matured further compared to day 3. The choriocapillaris, however, remained heavily fenestrated and free of tight junctions and vascular mural cells (Fig. 3 and Supplemental Fig. 3). At 5 dpf the choriocapillaris exhibited less fenestrations, a well-defined cytoplasm and mural cells were locally associated with the basal aspect of the vasculature, although the coverage was sparse (Fig. 3 and Supplemental Fig. 4). The Bruch's membrane was clearly defined, straight and thick, and the RPE and photoreceptor outer segments exhibited adult-like morphology and density (Fig. 3 and Supplemental Fig. 4). These findings demonstrate that, also at the ultrastructural level, maturation of the choriocapillaris, and associated structures, takes place late during larval development just prior to 120 hpf and provides structural evidence for the restriction of choriocapillaris sprouting in two-dimensions, required for generating its high density and lobular morphology.

3.6. Development of choroid rete mirabile during adolescence

Additional, posterior choroidal vascular networks are critical for regulating the flow through the choriocapillaris and may also serve other, as of yet poorly defined functions. The timing and mechanisms underlying their development is, however, poorly understood. In humans, the first seeds of these exterior choroidal vessels are planted early during human choroid development by posterior sprouting of the choriocapillaris (Lutty and McLeod, 2018), but we could not detect any such posterior sprouts in zebrafish during the first 120 h of development. By carefully analyzing cross-sections of the eye at adolescence (i.e. 4 weeks) and adult stages, it was clear that additional, exterior choroidal vessels were also present in zebrafish, but that these likely were developed at later stages of development (Fig. 4A). In particular, a thick multi-layered vasculature was clearly apparent in adults, underlying the choriocapillaris in the center of the optic disk, but this structure appeared to be poorly developed and thin at 4 weeks. It is known from histological examinations of other animals, including mammals that juxtaposed to the choriocapillaris, on the posterior side, a vasculature with characteristics of a “rete mirabile” is present with important functions in regulating exchange of gases, small chemicals or heat (Chung and Weon, 2008). Using Fli1a:EGFP fish, we performed careful dissection of the outer retinal layers and found that while a few endothelial cells had migrated posteriorly by 2 weeks post fertilization (wpf) and inhabited the area of the rete mirabile, the actual vascular network was not present in this region until at 3 wpf (Fig. 4B). From 3 wpf the rete mirabile was fully matured and appeared like in the adult fish (Fig. 4B), although still much smaller than in the adult (Fig. 4A). This vasculature also exhibited an extremely high density, resembling a tightly packed pile of bamboo-sticks typical for rete mirabile networks (Chung and Weon, 2008). The choriocapillaris, on the other hand, exhibited its terminal morphology and density already from 5 dpf onwards, suggesting that this vasculature matures much earlier than the rete mirabile.

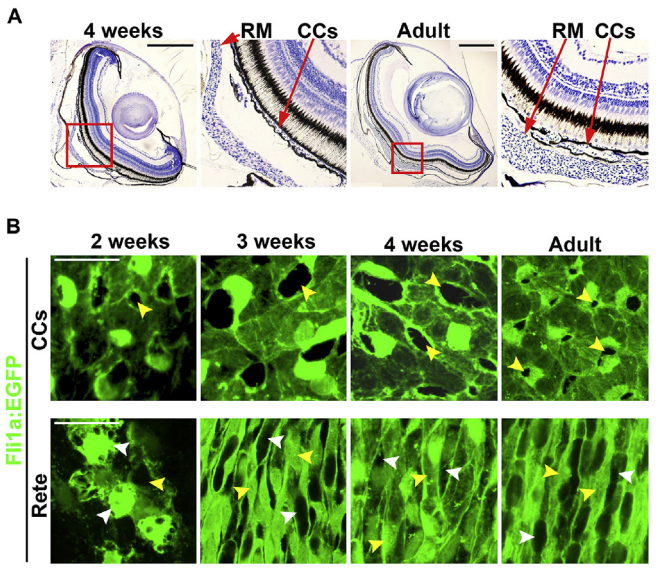

Fig. 4. Appearance of Rete Mirabile in the zebrafish during development. **A:** Bright field micrographs from cross sections of 4 weeks and adult zebrafish eyes stained with toluidine blue. The boxed regions are shown in the magnified images below. Size bars indicate 250 μm in each image. CCs. Choriocapillaries, RM. Rete Mirabile. **B:** Confocal micrographs of the choriocapillaris and Rete Mirabile from Fli1a:EGFP transgenic zebrafish (endothelium shown in green) at 2, 3, 4 weeks and adult stages. Yellow arrows indicate avascular area or interstitial foci and white arrows indicates vascular area. Size bars indicate 20 μm in each image.

3.7. Development of the choriocapillaris is dependent on VEGF-signaling via VEGFR2

Using newly developed genetically modified zebrafish strains in which various elements of the VEGF-signaling pathway have been manipulated, we set out to analyze the involvement of this pathway during choriocapillaris development. As hypoxia-signaling is one of the critical regulators of VEGF-production and angiogenesis during development and in disease (Jensen et al., 2011), we first investigated changes to choriocapillaris development in von Hippel-Lindau ($VHL^{-/-}$) mutants, in which hypoxia-signaling is enhanced due to the stabilization of hypoxia-inducible factor (HIF)-1α, alternatively in HIF1α knockout fish. As expected, $VHL^{-/-}$ fish exhibited markedly increased sprouting and growth of the choriocapillaris, evident as the presence of a higher number of smaller interstitial foci, leading to a higher vascular density compared to wildtype controls (Fig. 5A and B). On the other hand, $HIF1\alpha^{-/-}$ fish did not demonstrate any apparent change in choriocapillaris development suggesting that while enhanced HIF1α activity may lead to more VEGF-induced choroidal angiogenesis, baseline VEGF production is likely not dependent on HIF1α, alternatively that other VHL-targets may be involved in VEGF production at these early developmental stages (Fig. 5A and B). To investigate the role of VEGF-signaling directly, we next used VEGFR2a (Kdrl) and VEGFR2b (Kdr) knockout fish as well as a heat-shock inducible VEGF-loss of function strain in which a dominant negative version of VEGF-A is produced following heat shock. In both $VEGFR2a^{-/-}$ and $VEGFR2b^{-/-}$ fish, the angiogenic sprouting in the choriocapillaris was severely impaired as evident by the presence of fewer sprouts and fewer but much larger interstitial foci, leading to a markedly reduced density of the choriocapillaris. Similarly, overexpressing dominant negative VEGF-A from 24 hpf onwards also reduced the number of interstitial foci and density of the choriocapillaris (Fig. 5A and B). As both VEGF-A and VEGF-B signaling are impaired in VEGF-dominant negative fish, we used previously validated morpholinos (Jensen et al., 2015) to demonstrate that VEGF-A but not VEGF-B was responsible for impaired

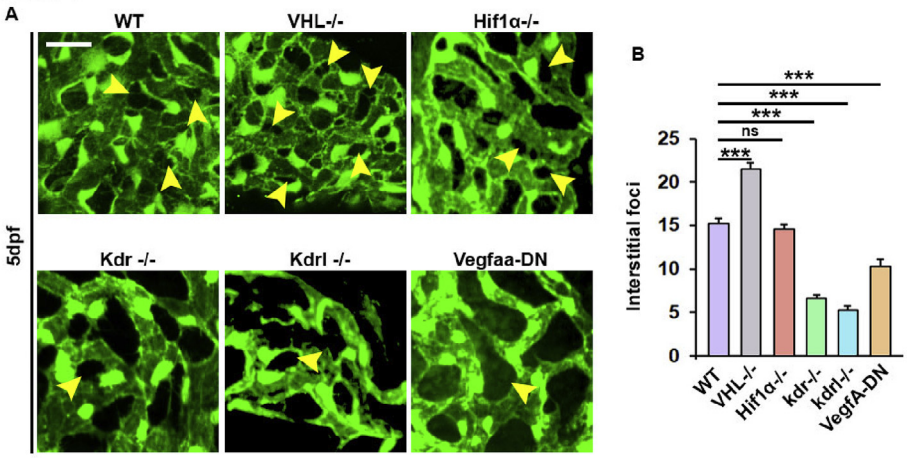

Fig. 5. Development of choriocapillaris is dependent on VEGF-VEGFR2 in zebrafish. A: Confocal micrographs of the choriocapillaris of 5 days post fertilization (dpf) embryos from wildtype (WT), VHL mutant (VHL$^{-/-}$), *hif1aa*$^{-/-}$;*hif1ab*$^{-/-}$ (HIF1a$^{-/-}$), *Vegfr2b*$^{-/-}$ (*kdr* $^{-/-}$), *Vegfr2a*$^{-/-}$ (*kdrl* $^{-/-}$) or fli1a:EGFP; Hsp70:Vegfaa-DN zebrafish incubated for 1 h at 37 °C daily from 1 to 5 dpf (Vegfaa-DN) crossed onto the Fli1a:EGFP background (endothelium shown in green). Yellow arrowheads indicate interstitial foci. Size bars indicates 20 μm in each image. **B:** Quantification of the number of interstitial foci in the experiment shown in **A.** n = 10–15 embryos, ***:p < 0.001. ns: non-significant.

choriocapillaris development (Supplemental Fig. 5). Interestingly, knocking down VEGF-A already from the one cell stage exhibited a stronger phenotype compared to inducing a pan-VEGF signaling blockade from 24 hpf onwards in the VEGF-dominant negative fish. Specifically, while EC migration into and within the outer eye field was not impaired in VEGF-A knockdown embryos, these ccECs failed to initiate vasculogenesis and remained as single ECs throughout development (Supplemental Fig. 5). At the concentrations of morpholino used in this study, other vasculatures forming by vasculogenesis including the aorta and cardinal vein appeared normal, although sprouting angiogenesis in the periphery was significantly impaired (Jensen et al., 2015). This implies that vasculogenesis in the choriocapillaris is more sensitive to reduced VEGF-A levels as compared to other vasculatures. Taken together, these findings demonstrate that VEGF-A signaling is a critical regulator of both early (vasculogenic) and late (sprouting angiogenic) choriocapillaris development in zebrafish.

3.8. VEGF-dependent delayed maturation is important for mouse choriocapillaris development

Next, using albino (BALB/c) mice, we investigated choriocapillaris formation and growth during embryonic and post-natal development and in adults by immunostaining with anti-CD31 antibodies, which specifically recognizing endothelial cells. Similar to the situation in zebrafish, an initial immature choriocapillaris exhibited marked two-dimensional angiogenic sprouting involving the entire vasculature starting at E12 (Fig. 6A). This remodeling phenotype continued into post-natal stages, suggesting that the delay in maturation is even more pronounced in mice compared to zebrafish. As such, stable number of interstitial foci were not reached until adulthood and these only increased slightly in number between E12 and P1 (Fig. 6A and B). From a gross morphology point of view, however, the mouse choriocapillaris was highly similar to that of the zebrafish both during development and in adults, and sprouting angiogenesis rather than intussusception also appeared to be the major mechanism involved in the expansion of the choriocapillaris in mice. To analyze the role of VEGFR2-signaling during choriocapillaris development in mice, we neutralized VEGFR2-signaling for three days by treatment at E12 with an anti-VEGFR2 neutralizing antibody followed by investigation of the choriocapillaris at E16. Similar to the findings in zebrafish, we observed a markedly reduced number of interstitial foci and sprouts, corresponding to a greatly reduced choriocapillaris vascular density in the VEGFR2-neutralizing antibody treated embryos compared to control IgG-treated embryos (Fig. 6C–E). Taken together, these results demonstrate that choriocapillaris development in both zebrafish and mice depend on ubiquitous and sustained VEGF-dependent sprouting leading to delayed maturation, which was required for endowing this vasculature with its uniquely high vascular density and 2-D sheet-like lobular morphology already from early developmental stages.

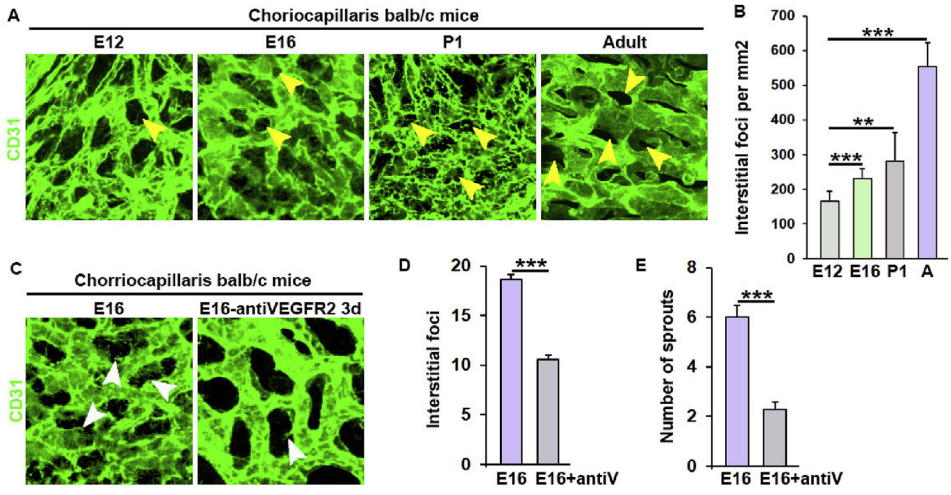

Fig. 6. Development of the choriocapillaris in mice is dependent of VEGFR2 signaling. A: Confocal micrographs of the choriocapillaris (CCs) from embryonic day (E)12, 16, postnatal day (P)1 and adult BALB/c mice stained with anti-CD31 (endothelium shown in green). Yellow arrowheads indicate interstitial foci. **B.** Quantification of the number of interstitial foci in the experiment shown in **A.** n = 10–15 areas of interest from four embryos collected from two litters, ***:p < 0.001, **:p < 0.005. A: Adult. **C.** Confocal micrographs of the choriocapillaris from E16 BALB/c mice treated with antiVEGFR2 neutralizing antibody or control IgG antibody for 3 days before staining with anti-CD31 antibody and visualization on the right side. **D:** Quantification of the number of interstitial foci in the experiment shown in **C.** n = 10–15 areas of interest from four embryos collected from two litters, ***:p < 0.001. antiV: Anti-VEGFR2-treated. **E:** Quantification of the number of sprouts in the experiment shown in **C.** n = 10–15 areas of interest from four embryos collected from two litters, ***:p < 0.001.

4. Discussion

The unique density and morphology of the choriocapillaris are critically involved in the development and maintenance of sight as well as development or progression of vision threatening disorders such as AMD, occurring when the tight regulation of ocular vascular homeostasis is disrupted (Luo et al., 2013; Cao et al., 2008). Reduced blood flow through the choriocapillaris in adults leads to outer retinal ischemia and is the key underlying factor for geographic atrophy of the photoreceptors and RPE, characterized in patients with “dry” AMD. On the other hand, pathological growth of the choriocapillaris outside of their 2-dimensional plane and into the RPE/retina underlies sub-retinal edema and hemorrhage characteristic of patients with “wet” AMD (Jager et al., 2008). In addition, the choriocapillaris is critically involved in the formation of the RPE, but also more distal structures during development (Zhang and Wildsoet, 2015). In spite of the importance of the choriocapillaris in health and disease, its unique morphology and the vast amount of studies investigating other ocular vasculatures (Jin et al., 2017; Connor et al., 2009), the mechanisms involved in the development of the choriocapillaris remains poorly understood.

In this work we present several novel insights into the mechanisms underlying choriocapillaris development. First, we show that the choriocapillaris form through vasculogenesis in a synchronized manner across the entire outer eye field. This synchronization was enabled by the preceding recruitment of single endothelial cells into the outer eye field, their aggregation into blood islands and the extension of endothelial processes connecting adjacent blood islands. This is to our knowledge the first time synchronized vasculogenesis has been demonstrated on a tissue-wide scale. In humans, blood islands were reported to form in the choroid and hyaloid prior to the development of choriocapillaris and hyaloid vasculature respectively (Lutty and McLeod, 2018; Lutty et al., 2010), suggesting that the synchronized vasculogenesis mechanism may be conserved in humans. Intriguingly, we show that erythroblasts were formed in these blood islands and existed in the premature choriocapillaris before the onset of perfusion through these vessels. This suggests that the choriocapillaris is a hematopoietic tissue during development. As the choriocapillaris is a much larger vasculature at these stages compared to other hematopoietic sites such as the hemogenic endothelium of the aorta or caudal hematopoietic plexus, this suggests that the choriocapillaris is a major contributor of erythroblasts in the early embryo. From approximately 36 hpf, the thin endothelial processes interconnecting adjacent blood islands developed into a primitive, non-lumenized vascular structure, which eventually became lumenized and perfused at 72 hpf. From the 36 hpf stage and onwards, the choriocapillaris mainly expanded by sprouting angiogenesis. Due to its unique morphology and density, it has been suggested that the choriocapillaris developed by intussusception, at least in birds (Djonov et al., 2000). However, carefully investigating numerous time-lapse videos captured between 3 and 5 dpf, we could not find evidence for intussusception, but ubiquitous sprouting which included neighboring endothelial cells and anastomosis of individual sprouts was evident. Our data does not rule out a role for intussusception in formation of the choriocapillaris, but we suggest that time-lapse or similar dynamic imaging techniques, in addition to morphological characterization, should be used to establish proof of intussusception during choriocapillaris development in future studies. Sprouting was sustained throughout development and across the entire choriocapillaris, and combined with delayed recruitment of perivascular mural cells and maturation of the endothelium in terms of tight junction formation and restricting fenestration. Similar persistent sprouting coupled to delayed maturation phenotypes was also observed in the mouse choriocapillaris during embryonic and early post-natal development. The zebrafish and mouse choriocapillaris matured at 120 hpf and post-natal stages respectively, when vision is enabled and becomes important for survival of the animal. VEGF-signaling via VEGFR2-induced PI3-kinase activation is critical for development of most vasculatures (Arbiser et al., 2007). Blocking VEGF-signaling through VEGFR2 during development, however, led to premature maturation and resulted in reduced vascular density in the choriocapillaris of both zebrafish and mice. Blocking VEGF production from the RPE in mice past E16 was found to be well tolerated and did not lead to reduced choriocapillaris density in adults (Le et al., 2010). As we demonstrate that the choriocapillaris was not fully developed at E16 in mice, it suggests that other signaling pathways may also be important and able to compensate for the lack of VEGF-A during choriocapillaris development. Previous studies have suggested that the choriocapillaris sprouts posteriorly, already from early stages of development in humans and mice (Lutty and McLeod, 2018; Le et al., 2010). In order to achieve the 2-dimensional, sheet-like morphology of the choriocapillaris, posterior sprouting, however, has to be regulated and reduced compared to lateral sprouting. However, how this is achieved has not been addressed in the past. We show here that choriocapillaris sprouting in zebrafish was restricted in the two-dimensional plane during embryonic and early larval development due to shielding by Bruch's membrane present at the retinal side, and a basement membrane present at the scleral side already from the onset of sprouting. This shielding did not allow choriocapillaries to grow into the retina or sclera at these stages. After the terminal morphology and density of the choriocapillaris had been achieved, however, the posterior inhibition was relieved leading to the development of other choroidal vasculature structures from 14 dpf onwards. We show here that the major of these additional choroidal vasculatures is a rete mirabile forming between 14 dpf and 1 mpf, and further growing in size until adult stages. Rete mirabile are very high density vascular networks with apparent functions related to exchange of gases, chemicals or heat from one compartment to another (Bataille et al., 2007). Rete mirabile vasculatures have also been found in the posterior eye/choroid of various other animals as well as occasionally humans. In humans, however, the development of rete mirabile in the choroid is associated with Moyamoya-disease complications in patients with a rare, but serious disorder known as PHACE syndrome (Chung and Weon, 2008; Rotter et al., 2018). Rete mirabile could also be a forerunner of hemangiomas (Lapidoth et al., 2009), which has been suggested in PHACE syndrome patients (Rotter et al., 2018). Rete mirabile vasculatures have never before been described in the zebrafish, but we expect that the discovery of these vessels in this important animal system may allow investigating their development in more detail. This may reveal novel mechanisms that could be targeted therapeutically for avoiding rete mirabile formation and thus treating patients with PHACE syndrome in the future.

5. Conclusions

In this work we demonstrate a new concept in developmental biology, namely the synchronized formation of a vasculature across an entire tissue by showing that the choriocapillaris is formed across the entire outer eye field by synchronized vasculogenesis. This was enabled by the recruitment and homogeneous interspersion of endothelial cells clustered within hematopoietic blood islands, which formed the basis for establishing the entire choriocapillaris in a single vasculogenic event between 36 and 48 hpf. We also demonstrate how the unique density and structure of the choriocapillaris is formed by ubiquitous and sustained sprouting angiogenesis within a two-dimensional plane, made possible by VEGF-induced delayed maturation of the vessels far beyond the stage where they become perfused with blood. Thirdly, we for the first time demonstrate the development of the choroidal rete mirabile, formed posterior to the choriocapillaris at the center of the optic disk in zebrafish from approximately 2 wpf. These novel findings shed new light on the mechanisms underlying the establishment of the choriocapillaris, a unique and poorly understood vasculature with key importance for regulation of sight in health and disease. We further expect this work will inspire the further use of zebrafish for understanding other aspects of choroidal vascular biology including the discovery of new targets for treatment of pathological choroidal vascular growth such as in patients with AMD or PHACE syndrome in the future.

Author contribution

ZA, DW, YY, RJ, XL, YC and LDJ designed research; ZA, DW, YY, DT-W and GV-R performed research; ZA, DW, YY, DT-W and LDJ analyzed data; GV-R, MM, RJ, XL and YC contributed vital new reagents or analytical tools; ZA and LDJ wrote the paper with input from all the authors.

Conflicts of interest

None declared.

Acknowledgements

We would like to thank the staff at the Zebrafish Core Facility, Center for Biological Resources at Linköping University for their excellent work maintaining our Zebrafish colonies in perfect breeding conditions. We are also deeply indebted to Prof. Markus Affolter (BioZentrum Basel) and Prof. Didier Stainier (Max Planck Institute, Bad Nauheim, Germany) for zebrafish lines used in this study and critical input that helped strengthen the interpretation of our findings. This work was supported by grants from Svenska Sällskapet för Medicinsk Forskning; Linköping Universitet; Eva och Oscar Ahréns Stiftelse; Ollie och Elof Ericssons Stiftelse; Stiftelsen Sigurd och Elsa Goljes Minne; Magnus Bergvalls Stiftelse; Ögonfonden; Jeanssons Stiftelser and Vetenskapsrådet. YY is supported by the National Natural Science Foundation of China (project No. 81773059) and by Shanghai Pujiang Program (project No. 18PJ1400600).

Appendix A. Supplementary data

Supplementary data to this article can be found online at https://doi.org/10.1016/j.ydbio.2019.02.002.

References

Alvarez, Y., Cederlund, M.L., Cottell, D.C., Bill, B.R., Ekker, S.C., Torres-Vazquez, J., Weinstein, B.M., Hyde, D.R., Vihtelic, T.S., Kennedy, B.N., 2007. Genetic determinants of hyaloid and retinal vasculature in zebrafish. BMC Dev. Biol. 7, 114.

Alvarez, Y., Astudillo, O., Jensen, L., Reynolds, A.L., Waghorne, N., Brazil, D.P., Cao, Y., O'Connor, J.J., Kennedy, B.N., 2009. Selective inhibition of retinal angiogenesis by targeting PI3 kinase. PLoS One 4, e7867.

Alvarez, Y., Chen, K., Reynolds, A.L., Waghorne, N., O'Connor, J.J., Kennedy, B.N., 2010. Predominant cone photoreceptor dysfunction in a hyperglycaemic model of non-proliferative diabetic retinopathy. Dis. Model Mech. 3, 236–245.

Arbiser, J.L., Kau, T., Konar, M., Narra, K., Ramchandran, R., Summers, S.A., Vlahos, C.J., Ye, K., Perry, B.N., Matter, W., Fischl, A., Cook, J., Silver, P.A., Bain, J., Cohen, P., Whitmire, D., Furness, S., Govindarajan, B., Bowen, J.P., 2007. Solenopsin, the alkaloidal component of the fire ant (Solenopsis invicta), is a naturally occurring inhibitor of phosphatidylinositol-3-kinase signaling and angiogenesis. Blood 109, 560–565.

Bataille, B., Wager, M., Lapierre, F., Goujon, J.M., Buffenoir, K., Rigoard, P., 2007. The significance of the rete mirabile in Vesalius's work: an example of the dangers of inductive inference in medicine. Neurosurgery 60, 761–768 discussion 8.

Cao, R., Jensen, L.D., Soll, I., Hauptmann, G., Cao, Y., 2008. Hypoxia-induced retinal angiogenesis in zebrafish as a model to study retinopathy. PLoS One 3, e2748.

Cao, Z., Jensen, L.D., Rouhi, P., Hosaka, K., Lanne, T., Steffensen, J.F., Wahlberg, E., Cao, Y., 2010. Hypoxia-induced retinopathy model in adult zebrafish. Nat. Protoc. 5, 1903–1910.

Chan-Ling, T., Koina, M.E., McColm, J.R., Dahlstrom, J.E., Bean, E., Adamson, S., Yun, S., Baxter, L., 2011. Role of CD44+ stem cells in mural cell formation in the human choroid: evidence of vascular instability due to limited pericyte ensheathment. Invest. Ophthalmol. Vis. Sci. 52, 399–410.

Chung, J.I., Weon, Y.C., 2008. Ophthalmic rete mirabile: the first angiographic documentation of embryonic ophthalmic collaterals in a patient with moyamoya disease. A case report. Intervent Neuroradiol. 14, 293–296.

Connor, K.M., Krah, N.M., Dennison, R.J., Aderman, C.M., Chen, J., Guerin, K.I., Sapieha, P., Stahl, A., Willett, K.L., Smith, L.E., 2009. Quantification of oxygen-induced retinopathy in the mouse: a model of vessel loss, vessel regrowth and pathological angiogenesis. Nat. Protoc. 4, 1565–1573.

Djonov, V., Schmid, M., Tschanz, S.A., Burri, P.H., 2000. Intussusceptive angiogenesis: its role in embryonic vascular network formation. Circ. Res. 86, 286–292.

Ellertsdottir, E., Lenard, A., Blum, Y., Krudewig, A., Herwig, L., Affolter, M., Belting, H.G., 2010. Vascular morphogenesis in the zebrafish embryo. Dev. Biol. 341, 56–65.

Gerri, C., Marin-Juez, R., Marass, M., Marks, A., Maischein, H.M., Stainier, D.Y.R., 2017. Hif-1 alpha regulates macrophage-endothelial interactions during blood vessel development in zebrafish. Nat. Commun. 8, 15492.

Gray, M.P., Smith, R.S., Soules, K.A., John, S.W., Link, B.A., 2009. The aqueous humor outflow pathway of zebrafish. Invest. Ophthalmol. Vis. Sci. 50, 1515–1521.

Hashiura, T., Kimura, E., Fujisawa, S., Oikawa, S., Nonaka, S., Kurosaka, D., Hitomi, J., 2017. Live imaging of primary ocular vasculature formation in zebrafish. PLoS One 12, e0176456.

Heinke, J., Patterson, C., Moser, M., 2012. Life is a pattern: vascular assembly within the embryo. Front. Biosci. (Elite Ed.) 4, 2269–2288.

Jager, R.D., Mieler, W.F., Miller, J.W., 2008. Age-related macular degeneration. N. Engl. J. Med. 358, 2606–2617.

Jensen, L.D., Rouhi, P., Cao, Z., Lanne, T., Wahlberg, E., Cao, Y., 2011. Zebrafish models to study hypoxia-induced pathological angiogenesis in malignant and nonmalignant diseases. Birth Defects Res. C Embryo Today 93, 182–193.

Jensen, L.D., Cao, Z., Nakamura, M., Yang, Y., Brautigam, L., Andersson, P., Zhang, Y., Wahlberg, E., Lanne, T., Hosaka, K., Cao, Y., 2012. Opposing effects of circadian clock genes bmal1 and period 2 in regulation of VEGF-dependent angiogenesis in developing zebrafish. Cell Rep. 2, 231–241.

Jensen, L.D., Nakamura, M., Brautigam, L., Li, X., Liu, Y., Samani, N.J., Cao, Y., 2015. VEGF-B-Neuropilin-1 signaling is spatiotemporally indispensable for vascular and neuronal development in zebrafish. Proc. Natl. Acad. Sci. U. S. A. 112, E5944–E5953.

Jin, S.W., Beis, D., Mitchell, T., Chen, J.N., Stainier, D.Y., 2005. Cellular and molecular analyses of vascular tube and lumen formation in zebrafish. Development 132, 5199–5209.

Jin, Y., Muhl, L., Burmakin, M., Wang, Y., Duchez, A.C., Betsholtz, C., Arthur, H.M., Jakobsson, L., 2017. Endoglin prevents vascular malformation by regulating flow-induced cell migration and specification through VEGFR2 signalling. Nat. Cell Biol. 19, 639–652.

Kaufman, R., Weiss, O., Sebbagh, M., Ravid, R., Gibbs-Bar, L., Yaniv, K., Inbal, A., 2015. Development and origins of Zebrafish ocular vasculature. BMC Dev. Biol. 15, 18.

Kikuchi, K., Holdway, J.E., Major, R.J., Blum, N., Dahn, R.D., Begemann, G., Poss, K.D., 2011. Retinoic acid production by endocardium and epicardium is an injury response essential for zebrafish heart regeneration. Dev. Cell 20, 397–404.

Lapidoth, M., Ben-Amitai, D., Bhandarkar, S., Fried, L., Arbiser, J.L., 2009. Efficacy of topical application of eosin for ulcerated hemangiomas. J. Am. Acad. Dermatol. 60, 350–351.

Lawson, N.D., Weinstein, B.M., 2002. In vivo imaging of embryonic vascular development using transgenic zebrafish. Dev. Biol. 248, 307–318.

Le, Y.Z., Bai, Y., Zhu, M., Zheng, L., 2010. Temporal requirement of RPE-derived VEGF in the development of choroidal vasculature. J. Neurochem. 112, 1584–1592.

Luo, L., Uehara, H., Zhang, X., Das, S.K., Olsen, T., Holt, D., Simonis, J.M., Jackman, K., Singh, N., Miya, T.R., Huang, W., Ahmed, F., Bastos-Carvalho, A., Le, Y.Z., Mamalis, C., Chiodo, V.A., Hauswirth, W.W., Baffi, J., Lacal, P.M., Orecchia, A., Ferrara, N., Gao, G., Young-Hee, K., Fu, Y., Owen, L., Albuquerque, R., Baehr, W., Thomas, K., Li, D.Y., Chalam, K.V., Shibuya, M., Grisanti, S., Wilson, D.J., Ambati, J., Ambati, B.K., 2013. Photoreceptor avascular privilege is shielded by soluble VEGF receptor-1. Elife 2, e00324.

Lutty, G.A., McLeod, D.S., 2018. Development of the hyaloid, choroidal and retinal vasculatures in the fetal human eye. Prog. Retin. Eye Res. 62, 58–76.

Lutty, G.A., Hasegawa, T., Baba, T., Grebe, R., Bhutto, I., McLeod, D.S., 2010. Development of the human choriocapillaris. Eye 24, 408.

Marin-Juez, R., Marass, M., Gauvrit, S., Rossi, A., Lai, S.L., Materna, S.C., Black, B.L., Stainier, D.Y., 2016. Fast revascularization of the injured area is essential to support zebrafish heart regeneration. Proc. Natl. Acad. Sci. U. S. A. 113, 11237–11242.

Rotter, A., Samorano, L.P., Rivitti-Machado, M.C., Oliveira, Z.N.P., Gontijo, B., 2018. PHACE syndrome: clinical manifestations, diagnostic criteria, and management. An. Bras. Dermatol. 93, 405–411.

Rouhi, P., Jensen, L.D., Cao, Z., Hosaka, K., Lanne, T., Wahlberg, E., Steffensen, J.F., Cao, Y., 2010. Hypoxia-induced metastasis model in embryonic zebrafish. Nat. Protoc. 5, 1911–1918.

Sauteur, L., Krudewig, A., Herwig, L., Ehrenfeuchter, N., Lenard, A., Affolter, M., Belting, H.G., 2014. Cdh5/VE-cadherin promotes endothelial cell interface elongation via cortical actin polymerization during angiogenic sprouting. Cell Rep. 9, 504–513.

Seiler, C., Abrams, J., Pack, M., 2010. Characterization of zebrafish intestinal smooth muscle development using a novel sm22alpha-b promoter. Dev. Dynam. 239, 2806–2812.

Traver, D., Paw, B.H., Poss, K.D., Penberthy, W.T., Lin, S., Zon, L.I., 2003. Transplantation and in vivo imaging of multilineage engraftment in zebrafish bloodless mutants. Nat. Immunol. 4, 1238–1246.

Whitesell, T.R., Kennedy, R.M., Carter, A.D., Rollins, E.L., Georgijevic, S., Santoro, M.M., Childs, S.J., 2014. An alpha-smooth muscle actin (acta2/alphasma) zebrafish transgenic line marking vascular mural cells and visceral smooth muscle cells. PLoS One 9, e90590.

Zhang, Y., Wildsoet, C.F., 2015. RPE and choroid mechanisms underlying ocular growth and myopia. Prog. Mol. Biol. Transl. Sci. 134, 221–240.

Zygmunt, T., Gay, C.M., Blondelle, J., Singh, M.K., Flaherty, K.M., Means, P.C., Herwig, L., Krudewig, A., Belting, H.G., Affolter, M., Epstein, J.A., Torres-Vazquez, J., 2011. Semaphorin-PlexinD1 signaling limits angiogenic potential via the VEGF decoy receptor sFlt 1. Dev. Cell 21, 301–314.